DESIGN AND DEVELOPMENT OF MULTILAYERED FUNCTIONALIZED ARTIFICIAL SKIN FOR PROSTHETIC APPLICATIONS: A BIOMIMETIC APPROACH

DOMINIKA ADAMCZYK^{1*} (ID., PIOTR SZATKOWSKI¹ (ID.), OLIWIA GRAŁEK² (ID., MARTYNA FRÖHLICH² (ID.), JUSTYNA MATYSEK² (ID.)

¹ DEPARTMENT OF GLASS TECHNOLOGY AND AMORPHOUS COATINGS, FACULTY OF MATERIALS SCIENCE AND CERAMICS, AGH UNIVERSITY OF KRAKOW, AL. MICKIEWICZA 30, 30-059 KRAKOW, POLAND

² DEPARTMENT OF BIOCYBERNETICS AND BIOMEDICAL ENGINEERING, FACULTY OF ELECTRICAL ENGINEERING, AUTOMATICS, COMPUTER SCIENCE AND BIOMEDICAL ENGINEERING, AGH UNIVERSITY OF KRAKOW, AL. MICKIEWICZA 30, 30-059 KRAKOW, POLAND

* E-MAIL: DADAMCZYK@AGH.EDU.PL

Abstract

The development of artificial skin for prosthetic applications poses a significant engineering challenge due to the need to replicate human skin's multilayered architecture and multifunctionality. Each layer must be engineered to mimic distinct skin functions including mechanical protection, thermal regulation, tactile sensation, and structural support. Additionally, the artificial skin must demonstrate biocompatibility, long-term durability, and seamless integration with prosthetic devices to provide users with enhanced sensory feedback and improved quality of life. This study aims to design and fabricate a low-cost, biomimetic four-laver artificial skin system using functionalized silicon composites to replicate human skin's multilayered architecture and multifunctional properties for prosthetic applications. The four-layer structure includes: a surface biomimetic porous layer for mechanical shielding, a thermal management layer enhanced with boron nitride fillers to improve heat conduction, a conductive sensing layer containing carbon nanotubes for pressure detection, and a base layer providing cushioning and structural integrity. Each layer was specifically engineered to mimic different skin functions: mechanical protection, thermal regulation, tactile sensation, and structural support. The total thickness of the fabricated layers matches the human skin thickness values. Mechanical characterization revealed properties compatible with prosthetic applications, while surface analysis confirmed successful texture modification for enhanced tactile interaction. The thermal layer demonstrated improved heat distribution capabilities, and the conductive layer showed potential for pressure sensing applications. This work presents a complete design approach for artificial skin that meets both appearance and functional needs for prosthetics. The developed system offers promising prospects for enhancing quality of life for amputees through improved sensory feedback and thermal comfort.

Keywords: artificial skin, biomimetic, layered, composites, tactile sensing, thermal management

[Engineering of Biomaterials 173 (2025) 12] doi:10.34821/eng.biomat.173.2025.12

Submitted: 2025-09-20, Accepted: 2025-10-27, Published: 2025-10-31



Copyright © 2025 by the authors. Some rights reserved. Except otherwise noted, this work is licensed under https://creativecommons.org/licenses/by/4.0

Introduction

The loss of skin function following amputation significantly impacts patients' quality of life, affecting aesthetic appearance, sensory perception, and thermal regulation [1]. In Poland alone, 10,560 lower limb and 1,099 upper limb amputations were reported in 2024, with over 8,400 patients receiving prosthetic limb reimbursement by government totalling 106 million PLN for lower limb prostheses and 6.6 million PLN for upper limb prostheses [2]. These figures align with global trends, where traumatic amputation incidence increased from 11.37 million cases in 1990 to 13.23 million in 2019 worldwide, with age-standardized incidence rates varying significantly across regions - from 101.01 per 100,000 in East Asia to 640.09 per 100,000 in Australasia [3]. Most frequently used prosthetic solutions mainly focus on mechanical functionality while lacking the complex sensory capabilities of natural skin. The development of artificial skin that can restore all these capabilities represents a critical advancement in prosthetic technology [4]. Human skin consists of three primary layers with distinct roles: the outer epidermis forms a thin but effective barrier withs prevents fluid loss and blocks bacterial invasion, the middle layer, dermis is well vascularized, houses touch, temperature, and pain receptors, and contains structures such as hair follicles and sweat glands while subcutaneous layer offers cushioning and isolation [5], [6]. The simplified skin model used for the skin substitute is presented in FIG 1.

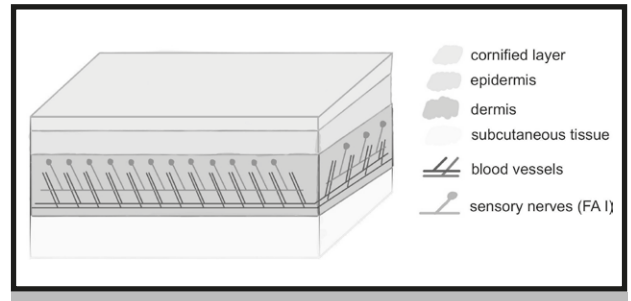


FIG. 1. Simplified skin model used for the manufacturing of a skin substitute.

Replicating this complex structure requires careful consideration of material selection, layer design, and functional integration [7], [8]. Recent advances in electronic skin (e-skin) technology have demonstrated the potential for creating materials that can sense pressure, temperature, and strain [9], [10]. Modern e-skins integrate self-healing materials that enable crack repair and recreate mechanical function. At the same time, next-generation systems incorporate artificial intelligence to optimize design and uncover user-personalized health profiles. [11], [12]. However, most current approaches focus on single-function sensors rather than multifunctional skin replacement systems. Combining multiple functions within a single artificial skin construct remains a significant engineering challenge. This study presents an approach to artificial skin design, incorporating biomimetic principles to create a multilayered system that addresses the primary functions of natural skin: protection, sensation, thermal regulation, and structural support [13]. The proposed four-layer architecture aims to replicate the hierarchical structure and multifunctional properties of human skin using cost-effective materials and manufacturing processes for prosthetic covering applications. This system is designed to restore essential sensory functions in prosthetic devices while maintaining economic accessibility for amputee patients.



Materials and Methods

The simplification assumed that the skin has no skin appendages, contains only one type of mechanoreceptor (FAI), and that blood vessels are the only factor contributing to the thermal properties of the skin. Concept of the manufactured skin substitute pointed in the FIG. 2., incorporating four distinct layers: surface layer mimicking the cornified layer and epidermis with controlled texture and porosity, functional thermal management layer simulating dermal vascular function, functional sensing layer representing mechanoreceptor functionality, and cushioning layer providing subcutaneous support.

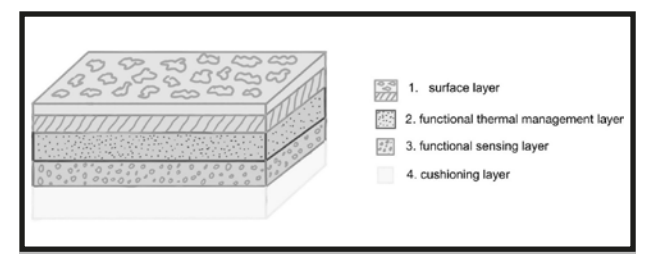


FIG. 2. Concept of the manufactured artificial skin: representation of the individual layers of the biomaterial construction, each corresponding to the analogous layers of natural skin.

Based on the simplified design representing the layered structure of the skin, an artificial skin model was created, the schematic of which is shown in FIG. 3. The artificial skin model was intended to reflect the layered organization of the skin, with each of its layers corresponding to the properties of the respective layers of human skin.

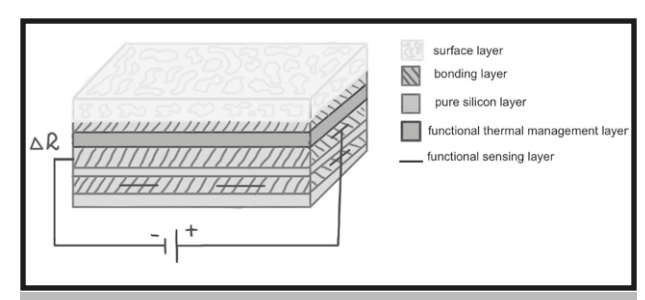


FIG. 3. Schematic illustrating the working principle and layer structure of the developed skin substitute composite.

During the design of artificial skin, the following materials were selected for its production. Condensation-cure RTV-2 silicone (Siliform 25, purchased from Ag-Bet) was selected as the base matrix due to its biocompatibility, flexibility, and ease of processing [14]. Functional modifications included adding: sodium bicarbonate (NaHCO₃) for surface texturing through controlled foaming, boron nitride (BN) for thermal conductivity enhancement, and multi-walled carbon nanotubes (MWCNT) for electrical conductivity [15].

The developed composite for prosthetic applications, shown in FIG. 4., consists of conductive layer that works by detecting resistance changes. When touched, the layer deforms, changing its resistance and the distance between MWCNTs, which affects electrical flow. The conductive layer is arranged in a grid (strips at different heights) to precisely detect touch location. Each layer was fabricated separately using casting techniques. The surface layer incorporated 25 wt% NaHCO₃ to create surface porosity and texture variation. The thermal layer utilized 20 wt%

BN particles dispersed through ultrasonic mixing to ensure uniform thermal property enhancement. The sensing layer employed carefully dispersed 2.5 wt% MWCNT to achieve electrical percolation while maintaining mechanical flexibility. The base layer consisted of pure silicone for structural support.

Briefly, the fabrication of the artificial skin began with precise weighing of uncrosslinked silicone using an analytical balance and distributing it into plastic beakers. Additives were prepared separately: colorants were added directly to silicone, BN or NaHCO₃ were weighed into beakers and then added to the non-crosslinked silicone (appropriate layers), while MWCNT were first ground in an agate mortar and subsequently ultrasonically homogenized with silicone using Cole-Parmer Ultrasonic Processor, amplitude 40-60 for 10 min total to prevent agglomeration. After homogenization, curing agent was added to each formulation in a ratio of 100:3 (silicone:curing agents) and mixed mechanically using mechanical stirrer CAT R100C, 900 rpm, for about 7 min, followed by casting the mixtures onto glass or Petri dishes to obtain uniform thin or thick layers depending on the additive. The samples were cured in a vacuum oven at 60 °C for 30 min and then left at room conditions overnight to complete crosslinking. Finally, layers were assembled using additional silicone as an adhesive interface. Surface preparation included controlled scoring to enhance interlayer adhesion. The assembly process was designed to prevent delamination while maintaining individual layer functionality. The complete artificial skin construct was evaluated for total thickness, layer integrity, and overall mechanical properties. Individual layer characterization included mechanical testing, surface analysis, and functional assessment relevant to each layer's intended purpose.

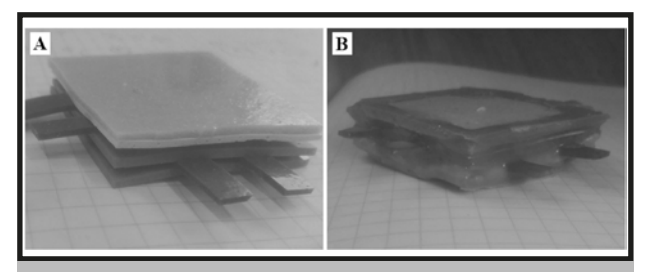


FIG. 4. Fabricated skin substitute layers: A – before bonding, B – after bonding.

Results and Discussions

Characterization of the obtained material started with thickness measurements of the formed layers (FIG. 5.). Thickness measurements were performed using a micrometer caliper (measurement range: 0-25 mm, resolution: 0.01 mm). For pure silicone, measurements were taken for both thinner and thicker variants, resulting in a total of five analysed layers. Each layer was measured at ten different points across its surface to ensure accuracy and reproducibility. The thickness measurement analysis revealed significant variations depending on layer composition. The highest result variability was observed for the layer containing 25% NaHCO₃, while the addition of porogen to pure silicone increased layer thickness. Particularly interesting behavior was noted for layers with 20% BN and 2.5% MWCNT, which, despite identical spreading thickness as the reference silicone, showed substantial final thickness reductions of 40% and 19%, respectively. This may be attributed to the interaction between fillers and silicone matrix during curing, where BN and MWCNT particles can influence

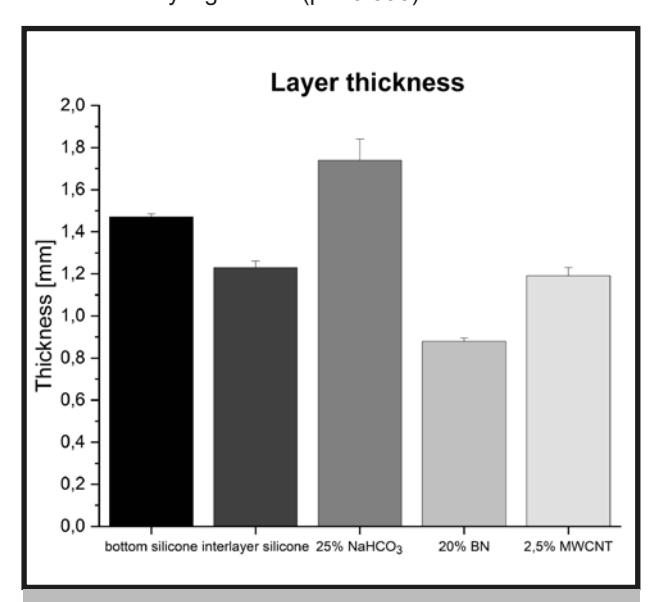


FIG. 5. The thickness measurement results of each layer.

Microscopic observations of the microstructure of the fabricated lavers were performed using a Kevence VHX-5000 digital microscope. The automatic shutter speed adjustment mode was applied to obtain optimal image brightness. Microscopic analysis shown in FIG 6. and 7. confirmed successful layer integration without delamination. Surface examination of the side revealed distinct morphological characteristics across different formulations. Pure silicon layers exhibited isolated shallow surface pores, while layers containing 20% BN demonstrated uniform surfaces with minimal contamination. The 25% NaHCO₃ formulation showed irregularly distributed pores of varying diameters on the surface. Layers with 2.5% MWCNT displayed darker points and exhibited a color change from dark blue to gray despite the absence of dye. In contrast, dyed layers maintained a light green coloration, with BN-containing samples showing a brighter green shade. Cross-sectional analysis revealed porosity in all layer types, with 25% NaHCO₃ samples exhibiting the highest pore volume. Notably, MWCNTcontaining layers showed increased porosity compared to pure silicon despite lacking a porogen. Adhesion properties, influenced by the casting method (silicon poured onto glass), varied significantly: pure silicon separated cleanly from glass surfaces, while 20% BN and 2.5% MWCNT layers demonstrated adhesion difficulties, evidenced by surface microstructural damage during removal. The 25% NaHCO₃ formulation, despite developing porosity at the glass interface, separated successfully due to the application of silicone.

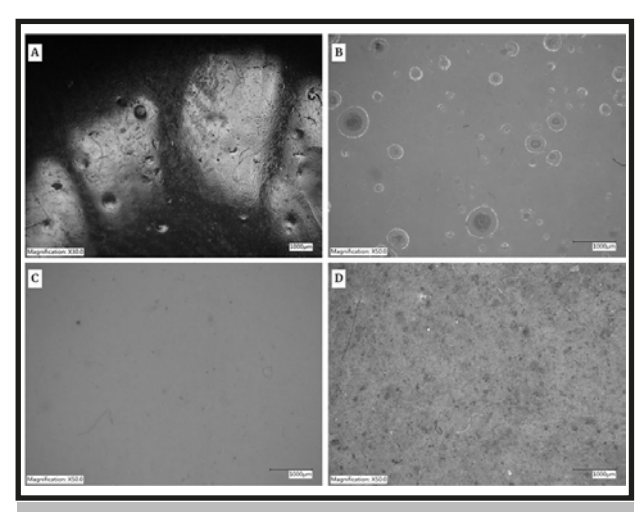


FIG. 6. Microscopic images: A – pure silicone, B – silicone with 25% NaHCO₃, C – silicone with 20% BN, D – silicone with 2.5% MWCNT.

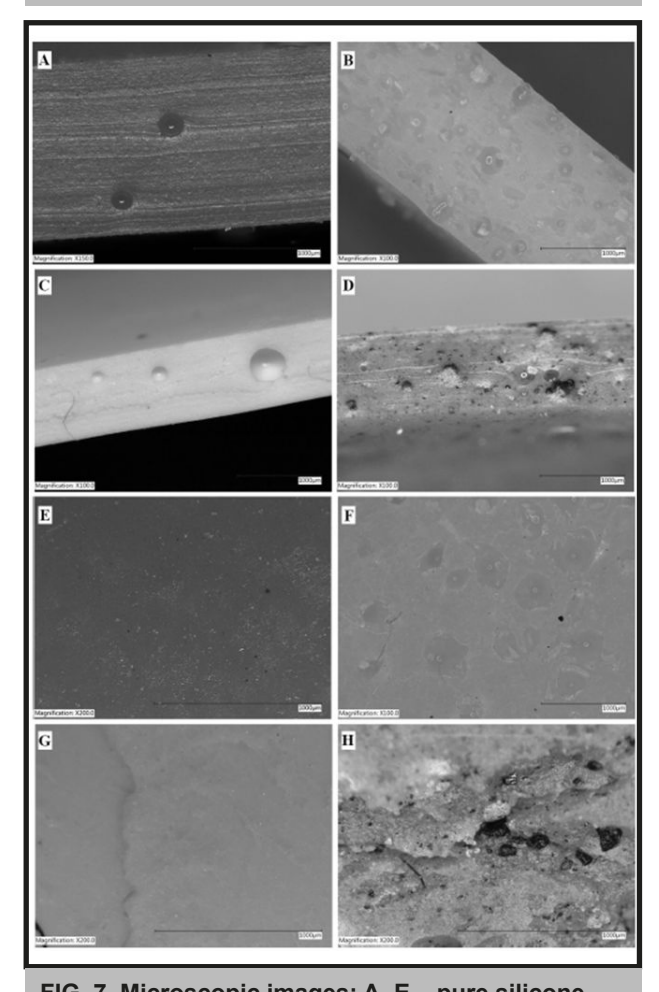


FIG. 7. Microscopic images: A, E – pure silicone, B, F – silicone with 25% NaHCO $_3$, C, G – silicone with 20% BN, D, H – silicone with 2.5% MWCNT.

Surface roughness is defined as the presence of optical or mechanical irregularities with small spatial separations on a material's surface. Surface topography of the fabricated layers was analysed on both sides using a Hommel Tester T1000 (HOMMELWERKE) static profilometer with Turbo Datawin-NT 1.45 software. Cross-sectional examination shown in FIG 8. revealed distinct layer boundaries while maintaining structural continuity. Pure silicon exhibited low roughness parameters on both glass-adjacent and air-exposed surfaces, with Ra values of 0.2 μ m, Rz of 1.7 μ m, and Rt of 3 μ m

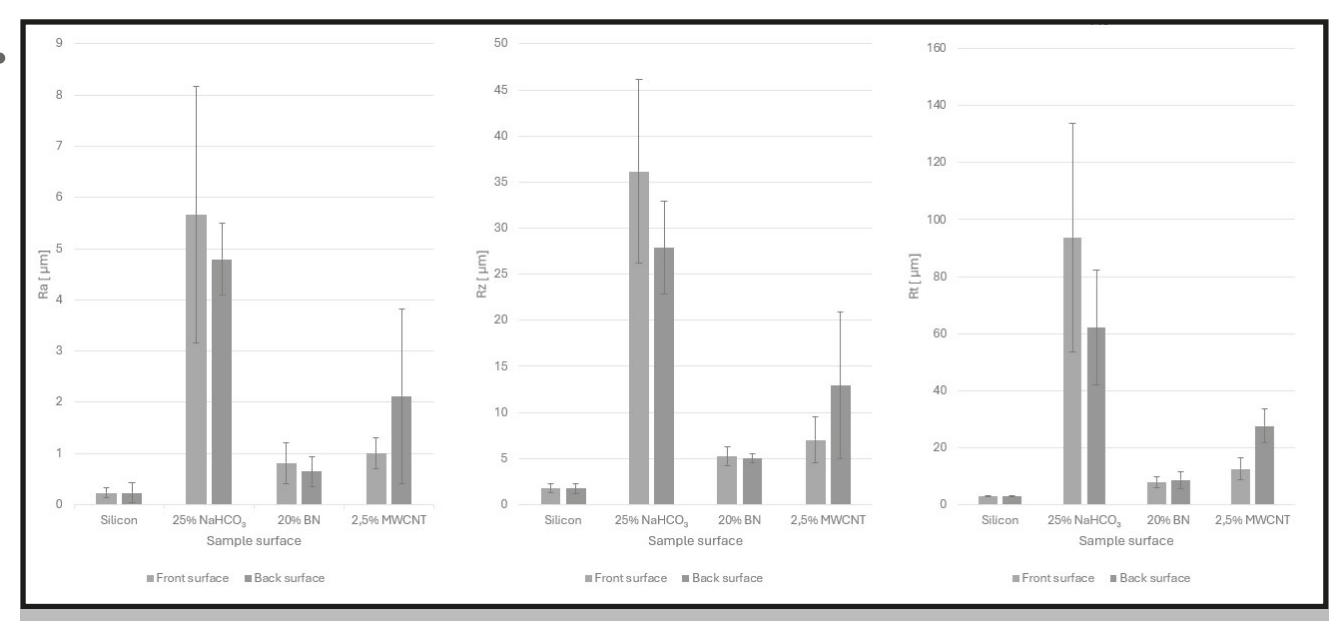


FIG. 8. Profilometry parameters for fabricated layers with standard deviation: A – Ra parameter, B – Rz parameter, C – Rt parameter.

on both sides. Following additive incorporation, all layers maintained Ra values below 1 µm, except for 25% NaHCO₃ and 2.5% MWCNT layers on the glass-side surface, which showed increased parameters. The 20% BN additive had minimal impact on surface roughness compared to other additives, though the glass-adjacent surface showed more individual elevations with higher peak values (Rt parameter). The 2.5% MWCNT formulation demonstrated significant roughness changes on the glass-side surface, with Ra and Rz parameters reaching twice the values of pure silicon and exhibiting large standard deviations, indicating highly irregular surfaces. The most pronounced changes occurred in the 25% NaHCO₃ layer, which showed the highest parameter variations across all three measurements, with Rt values exceeding pure silicon by over 80 µm. This formulation achieved the greatest surface roughness among all tested layers, with the highest standard deviation on the air-exposed surface, though the roughness profile did not resemble human skin characteristics due to insufficient Ra and Rz values [21]. All three roughness parameters (Ra, Rz, Rt) showed highly significant differences between materials. The Ra parameter analysis (F = 40.833, p < 0.001) revealed that 25% NaHCO₃ produced the highest surface roughness, significantly different from all other materials except for the non-significant comparison between 20% BN and 2.5% MWCNT (p = 0.124). The Rt parameter showed the most dramatic differences (F = 267.186, p < 0.001), with 25% NaHCO₃ exhibiting values exceeding 80 µm, substantially higher than other materials.

A surface wettability study was subsequently conducted. Contact angle measurements were performed at room temperature using a DSA 10 Mk2 goniometer (Krüss). The measurements were acquired with the instrument's dedicated DSA software at a magnification of x20. For each of the four fabricated layers, ten droplet measurements were carried out. All four tested layers exhibited hydrophobic surface characteristics. Following the addition of additives, the hydrophobic character decreased, however the materials remained hydrophobic. The pure silicone layer showed a contact angle of 111.3°. With the addition of 25% NaHCO₃ pore-forming agent, the angle decreased by 0.89%. This layer displayed a large standard deviation, indicating the influence of pores on contact angle measurements. The addition of 20% BN reduced the contact angle by 4.13% compared to pure silicone. 2.5% MWCNT decreased the angle by 4.58%, achieving the lowest contact angle value. Similar to the 25% NaHCO3 layer, the 2.5% MWCNT layer showed large standard deviation, indicating significant result scatter. The analysis revealed significant differences between materials (F = 6.059, p = 0.002). Pure silicone showed significantly higher contact angles compared to both 20% BN and 2.5% MWCNT additives (p < 0.001 for both comparisons), indicating that these additives effectively reduced the hydrophobic character of the silicone matrix. The comparison between 25% NaHCO₃ and pure silicone was not statistically significant despite the 0.89% reduction. The results are presented in FIG. 9. The contact angle values were higher than those of skin. Under normal conditions, skin exhibits hydrophilic character with contact angles ranging from 50-70°. Skin can achieve contact angle values of 120°, exceeding the obtained results for the tested layers, but only after thorough cleaning and washing with soap [22].

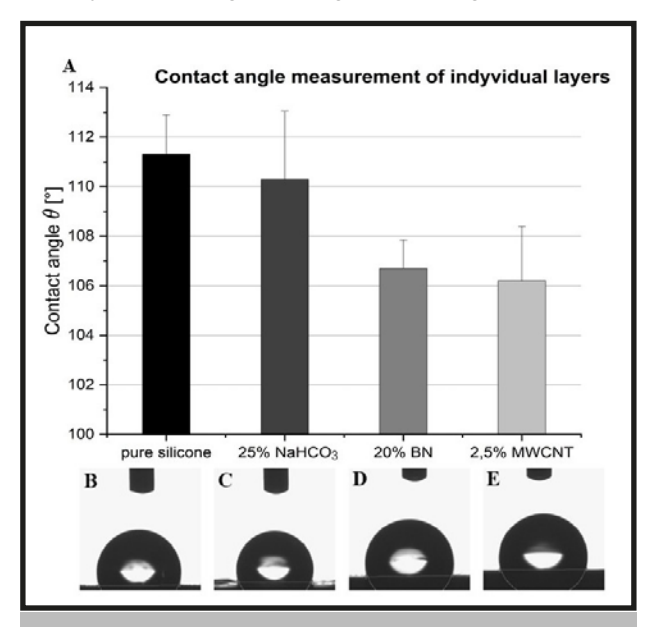


FIG. 9. Contact angle measurements: A – results for individual layers with standard deviation and percentage variation, B – droplet from pure silicone measurement, C – silicone with 25% NaHCO₃, D – silicone with 20% BN, E – silicone with 2.5% MWCNT.

Conclusions

This study successfully demonstrated the feasibility of creating a multilayered artificial skin system using functionalized silicone composites. The biomimetic design approach effectively addressed the primary functional requirements of prosthetic skin applications: surface texture for tactile interaction, thermal management for comfort, pressure sensing capability, and structural support. The developed artificial skin construct represents a significant step toward comprehensive skin replacement systems for prosthetic applications. The modular design approach enables optimization of individual layer properties while maintaining overall system integration. Future work should focus on electronic integration, long-term durability assessment, and clinical validation for prosthetic applications. The results provide

a foundation for advanced artificial skin development, with potential applications extending beyond prosthetics to include wearable sensors, medical monitoring devices, and soft robotics applications. The findings are highly promising and suggest that the proposed system could serve as a solid basis for further experimental studies. These results may guide future efforts in the development and refinement of fully functional artificial skin.

Acknowledgments

This work was supported from the subsidy of the Ministry of Education and Science for the AGH University of Science and Technology in Kraków (Project No. 16.16.160.557). The authors gratefully acknowledge Prof. Kinga Pielichowska for her valuable scientific advice and support.

References

- [1] Yu J.R., Navarro J., Coburn J.C., Mahadik B., Molnar J., Holmes J.H., Nam A.J., Fisher J.P.: Current and Future Perspectives on Skin Tissue Engineering: Key Features of Biomedical Research, Translational Assessment, and Clinical Application. Adv. *Healthc*. Mater. 8 (2019) 1801471. [2] Osborn L., Nguyen H., Betthauser J., Kaliki R., Thakor N.: Biologically inspired multi-layered synthetic skin for tactile feedback in prosthetic limbs. *Proc. IEEE Eng. Med. Biol. Soc.* (2016) 4622–4625.
- [3] Han Y., Lv S., Hao C., Ding F., Zhang Y.: Thermal conductivity enhancement of BN/silicone composites cured under electric field: Stacking of shape, thermal conductivity, and particle packing structure anisotropies. *Thermochim.* Acta 529 (2012) 68–73.
- [4] So H.M., Sim J.W., Kwon J., Yun J., Baik S., Chang W.S.: Carbon nanotube based pressure sensor for flexible electronics. *Mater. Res. Bull.* 48 (2013) 5036–5039.
- [5] Brohem C.A., Da Silva Cardeal L.B., Tiago M., Soengas M.S., De Moraes Barros S.B., Maria-Engler S.S.: Artificial Skin in Perspective: Concepts and Applications. *Pigment Cell Melanoma Res.* 24 (2010) 35–50.
- [6] Igarashi T., Nishino K., Nayar S.K.: The Appearance of Human Skin. (2005).
- [7] Humbert P., Maibach H.I., Fanian F., Agache P.: Agache's Measuring the Skin: Non-invasive Investigations, Physiology, Normal Constants. Springer, Cham 2017.
- [8] Sinha R., Van Den Heuvel J.A.: A systematic literature review of quality of life in lower limb amputees. *Disabil. Rehabil.* 33 (2011) 879–888.
- [9] Amputacje i protezy 2020–2024. Available online: https://ezdrowie.gov.pl/23908 (accessed 14 August 2025). [10] Yuan B., Hu D., Gu S., Xiao S., Song F.: The global burden of traumatic amputation in 204 countries and territories. Front. Public Health 11 (2023) 1258853.
- [11] Cordella F., Ciancio A.L., Sacchetti R., Davalli A., Cutti A.G., Guglielmelli E., Zollo L.: Literature review on needs of upper limb prosthesis users. *Front. Neurosci.* 10 (2016) 209.

- [12] MacNeil S.: Progress and opportunities for tissue-engineered skin. *Nature* 445 (2007) 874–880.
- [13] Schmid G., Cecil S., Überbacher R.: The role of skin conductivity in a low frequency exposure assessment for peripheral nerve tissue according to the ICNIRP 2010 guidelines. *Phys. Med. Biol.* 58 (2013) 4703–4716.
- [14] Xu C., Solomon S.A., Gao W.: Artificial Intelligence-Powered Electronic Skin. *Nat. Mach. Intell.* 5 (2023) 1344–1356.
- [15] Chen J., Wang L., Xu X., Liu G., Liu H., Qiao Y., Chen J., Cao S., Cha Q., Wang T.: Self-Healing Materials-Based Electronic Skin: Mechanism, Development and Applications. *Gels* 8 (2022) 356.
- [16] What are RTV-2 Silicones? Elkem. Available online: https://www.elkem.com/products/silicones/rtv-2 (accessed 13 July 2025).
- [17] Kong S.M., Mariatti M., Busfield J.J.C.: Effects of types of fillers and filler loading on the properties of silicone rubber composites. *J. Reinf. Plast. Compos.* 30 (2011) 1087–1096.
- [18] Gulotty R., Castellino M., Jagdale P., Tagliaferro A., Balandin A.A.: Effects of Functionalization on Thermal Properties of Single-Wall and Multi-Wall Carbon Nanotube—Polymer Nanocomposites. arXiv preprint (2013). Available online: https://arxiv.org/pdf/1305.3822 (accessed 20 August 2025).
- [19] Teng C.C., Ma C.C.M., Chiou K.C., Lee T.M., Shih Y.F.: Synergetic effect of hybrid boron nitride and multi-walled carbon nanotubes on the thermal conductivity of epoxy composites. *Mater. Chem. Phys.* 126 (2011) 722–728.
- [20] Kumar V., Alam M.N., Manikkavel A., Song M., Lee D.J., Park S.S.: Silicone Rubber Composites Reinforced by Carbon Nanofillers and Their Hybrids for Various Applications: A Review. *Polymers* 13 (2021) 2322.
- [21] Potorac A.D., Toma I., Mignot J.: In vivo skin relief measurement using a new optical profilometer. *Skin Res. Technol.* 2 (1996) 64–69.
- [22] Ginn M.E., Noyes C.M., Jungermann E.: The contact angle of water on viable human skin. *J. Colloid Interface Sci.* 26 (1968) 146–151.

SICH MERING OF

.